Potential Correlations between Apparent Peaks in LENR Transmutation Data and Deuteron Fusion Screening Data

David J. Nagel
George Washington University, USA
nagel@gwu.edu

Abstract

Diverse experiments have been performed during the study of Low Energy Nuclear Reactions (LENR) since the 1989 announcement and paper by Fleischmann and Pons. Data from two very different LENR transmutation experiments each show five peaks, which occur at the same locations as a function of atomic mass. A compilation plot of about one hundred measured screening potential energies from deuteron fusion nuclear reactions at relatively low beam energies was made as a function of atomic number. The data scatter significantly, but still exhibit five peaks at the same locations as the transmutation data. The origins of the peaking in the transmutation and in the fusion screening data are not understood. Neither is the correlation of the peak locations in the two widely diverse types of LENR experiments. Explanation of the peaks and correlations might contribute to the understanding of LENR.

1. Introduction.

Over one-third of a century of research on Low Energy Nuclear Reactions has produced a remarkable amount of experimental data. Examination of some of that data revealed an unexpected potential correlation between the transmutation data and the screening energies from low-beam-energy deuterium fusion experiments. The five peaks that occur in both data sets all align with each other as a function of atomic mass. Further, a theoretical calculation of neutron absorption by an optical potential model, also as a function of atomic mass, gives peaks at the same five values of atomic mass.

This paper reviews the experimental and theoretical data, notes the discovery of the correlation, and discusses its implications. The next section summarizes the optical model calculations, which plays a significant role in the discussion. They clearly show the five peaks and their locations at specific values of atomic mass. Then, the two transmutation experiments are described and their results are compared in Section 3. The following section reviews deuteron fusion experiments at beam energies of a few keV. Section 5 contains compilations of screening potential energies that are extracted from the measured fusion rates and cross sections. The correlations between the transmutation and fusion reaction data sets are presented in Section 6. As if the alignment of peaks in the transmutation and screening data were not enough of a puzzle, we also note in Section 7 that the peaks in those data sets also align with data from very different muon capture experiments. The final section includes a discussion of the new correlation, and its relationship to the distribution of elements in Nature. The possibility that the potential correlations noted and discussed in this paper could have been discovered by modern Artificial Intelligence tools is also noted in the final section.

2. Optical Model Calculation.

Larsen founded Lattice Energy LLC in Chicago in 2001. The company sought to understand and exploit what were originally called "cold fusion" experiments. He funded Miley at the University of Illinois to perform such experiments. They showed very interesting results across most of the periodic table. That motivated Larsen to fund Widom at the Northeastern University to consider the transmutation results, and try to explain them theoretically.

Widom and Larsen developed a theory for the mechanism behind experiments that we will henceforth call LENR experiments. In 2005, they published their concepts and results obtained with them[1]. Part of the abstract of that paper describes their results:

> Weak interaction catalysis initially occurs when neutrons (along with neutrinos) are produced from the protons which capture 'heavy' electrons. Surface electron masses are shifted upwards by localized condensed matter electromagnetic fields. No Coulomb barriers exist for the weak interaction neutron production or other resulting catalytic processes.

When it was published, the Widom-Larsen theory was one of the more sophisticated discussions of why and how LENR occur.

Widom and Larsen published a sequel to their original paper in 2007[2]. That more detailed paper contained two especially interesting results. One is specific predicted nuclear reaction rates per square centimeter. The other is the magnitude of their "localized condensed matter electromagnetic fields". It was given as about 100 V per nanometer, a value so high as to be bothersome to critics of the theory. Negative critiques of the Widom-Larsen theory were published by Hagelstein and Chaudhary in 2008[3] and by Vysotskii in 2014[4]. Widom and Larsen rebutted the Hagelstein-Chaudhary criticism in a 2008 paper[5]. That year, Srivastava, Widom, and Larsen posted a paper[6] on the ArXiv server entitled "A Primer for Electro-Weak Induced Low Energy Nuclear Reactions", which was published two years later[7]. In 2015, Larsen posted a set of 133 graphics described as an index to the Widom-Larsen theory[8]. It is a wide-ranging review of both the theory and its several applications. In 2019, Larsen posted a White Paper[9] about the application of their theory to "green radiation-free nuclear power and propulsion.**"**. Larsen died that year[10]. It appears that his theory with Widom is no longer getting attention, either theoretically or experimentally.

Early in the 2001-2019 period of activity by Larsen and his colleagues, Widom and Larsen posted another theoretical paper on the ArXiv server[11]. That 2006 article is central to the discussions in this paper. It was entitled "Nuclear Abundances in Metallic Hydride Electrodes of Electrolytic Chemical Cells". The abstract reads in part:

> Low energy nuclear transmutations have been reported in experimental chemical electrolytic cells employing metallic hydride electrodes. Assuming that the nuclear transmutations are induced by ultra-low momentum neutron absorption, the expected chemical cell nuclear abundances are discussed on the basis of a neutron optical potential model. The theoretical results are in satisfactory agreement with available experimental chemical cell data.

The paper considers a spherical nuclear potential, where the well radius R for a given atomic mass number A is $R = aA^{1/3}$ with $a = 1.2 \times 10^{-15}$ m.

The 2006 paper contained three figures. The first has the results of the optical model calculation, which were denoted f(A). The other two figures included that curve with overplots of experimental data from Miley and Patterson. Those data are presented and referenced in the next section. Figure 1 is one of the latter Widom-Larsen plots. It shows that the peaks in the theoretical neutron cross section plot tend to align with higher values in the widely scattered measured LENR rates. The peaks occur at atomic mass units (AMU) of 12, 32, 66, 120 and 198. Those mass values, and their atomic number equivalents, come up again in the following sections on transmutation and deuteron fusion results.

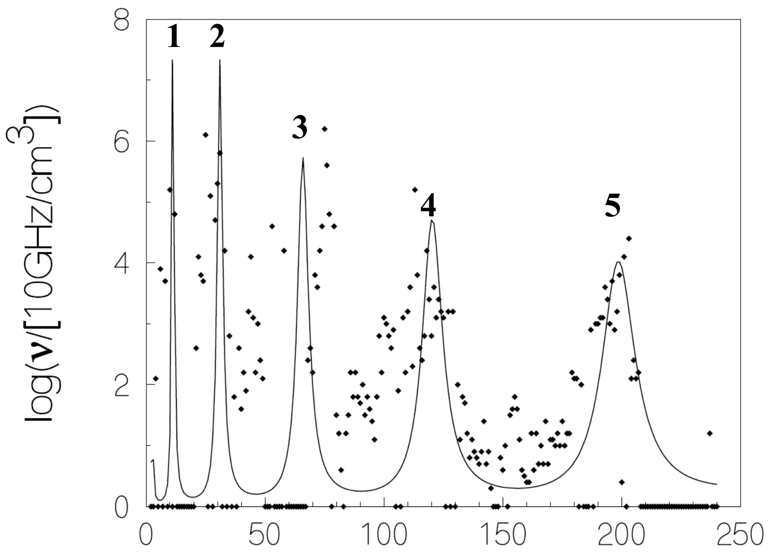

Figure 1. Plot of the nuclear rate in reactions per second per cubic centimeter measured by Miley and Patterson (the points) and the Widom-Larsen theoretical optical model f(A)

The authors of the 2006 paper make three statements that are relevant to the observations and implications discussed in this paper. The quotations follow, not in the published order:
It must be noted that the apparent alignment of the theoretical model with the data from Miley and Patterson is not a validation of the basic Widom-Larsen theory. Their theory posits that interactions of electrons with very high electromagnetic fields, which are caused by surface waves, result in heavy electrons, which interact with deuterons (or protons) to produce "ultra-low momentum" neutrons. Those neutrons then cause LENR with nearby nuclei.

The fitting of neutron wavelengths into spherical nuclei, as touted by Widom and Larsen in discussing their Optical Potential model, enables an interesting calculation. It leads to a plot of the computed diameter of the nuclei at the atomic masses of the peaks vs the peak number, 1 through 5. That plot is in Figure 2. As noted in the caption, the resulting neutron wavelength

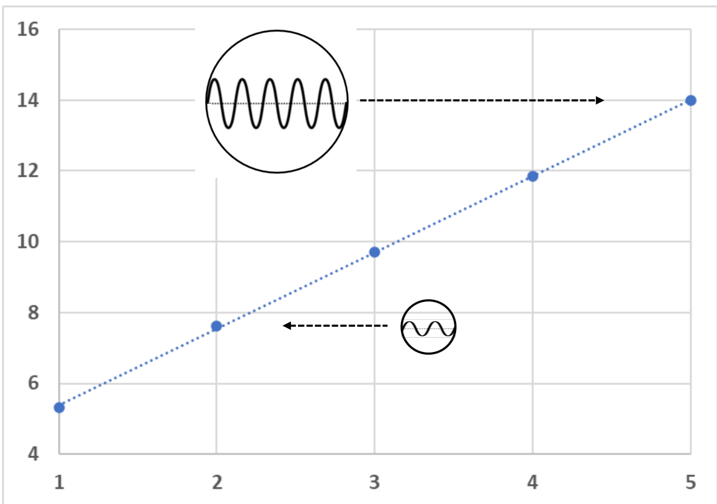

Figure 2. Relationship of the nuclear diameter D in femtometres vertically as a function of the numbers N of the peaks in Figure 1. The insets are cartoons of the fits for the second and fifth peaks. The equation for the line is $D = 2.154\ N + 3.234$ with $R^2 = 0.9998$. Hence, the plot gives the neutron wavelength in nuclear matter as 2.154 fm.

in nuclei is 2.154 fm. An independent determination of that wavelength has not been found. Interestingly, the diameter of a neutron is about 1.67 fm[12].

In short, Widom and Larsen attribute peaks in the transmutation data to an integral number of the wavelengths of neutrons within nuclei fitting into nuclei of various radii. They also note that "Very remarkably, the product yield in a chemical cell is in some ways qualitatively similar to nuclear abundances found in our local solar system and galaxy". A review of heavy element synthesis was cited to back up that statement[13]. We will return to the topic of natural distributions (abundances) of elements in the penultimate section.

3. Transmutation Experiments and Data

There have been many reports of elements produced by LENR. Most of that transmutation data involves light element products. However, there are three comprehensive transmutation data sets, each with data on elemental production across the periodic table. We will introduce them briefly in the next sub-section. Then we will compare them with each other, and with the optical model calculations that were reviewed in the preceding section. The associated with the data sets and the relationships are shown in Figure 3.

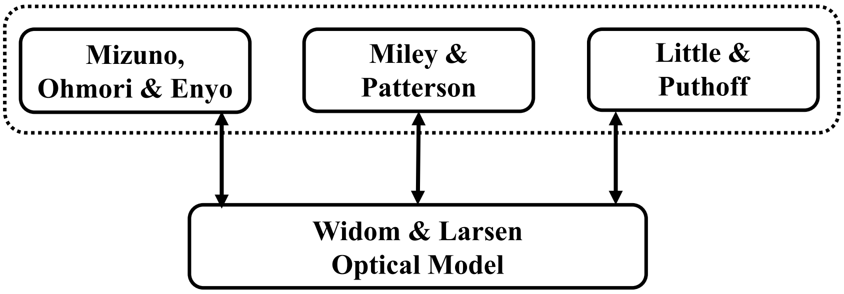

Figure 3. Three large transmutation data sets, and the comparisons among them (dashed box) and comparisons with the Optical Model of Widom and Larsen (arrows).

A. Transmutation Experiments

The laboratory setups for some of the transmutation experiments are very different, as shown in Figure 4. Mizuno and his colleagues used a sealed electrolysis system, while both of the other experiment involved the flow of electrolytes through beds of metal-coated plastic spheres. The several papers written by the scientists, who performed the three transmutation studies, are long and detailed. Brief summaries of what they did follow.

(1) Mizuno, Ohmori and Enyo Experiments.

Mizuno and his collaborators in Hokkaido presented results from an unusual LENR experiment[14]. They electrolyzed a Pd rod in a closed cell containing a heavy water (D_2O) electrolyte at high pressures, temperatures, and current densities for 32 days. They used four analytical techniques, Secondary Ion Mass Spectrometry, Auger Electron Spectroscopy, Energy Dispersive X-Ray Spectroscopy, and Electron Probe Microanalysis. Data were reported as count rates from Secondary Ion Mass Spectrometry. The Mizuno data are from post-run analyses, and not the difference of pre- and post-run values. These data were published in 1996.

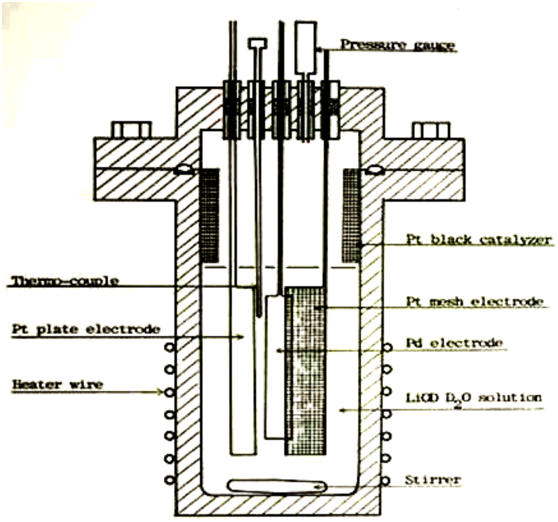

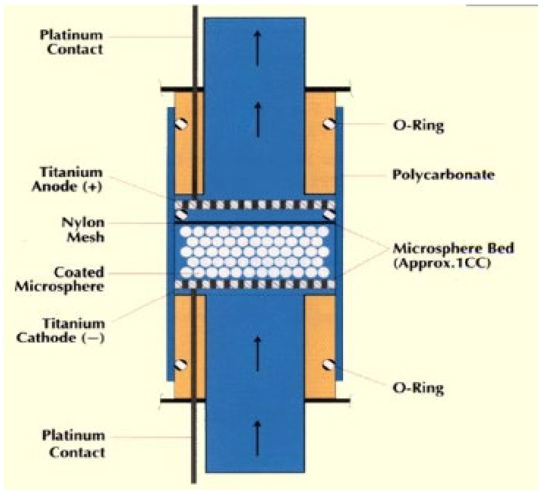

Figure 4. Left: A schematic of the experiment by Mizuno, Ohmori and Enyo. Right: A drawing of the experiments by Miley and Patterson, and by Little and Puthoff.

(2) Miley and Patterson Experiments.

Also in 1996, Miley in The University of Illinois (UI) published data from a unique LENR experiment using materials from Patterson[15]. They electrolyzed plastic beads coated with Pd and Ni in a packed bed configuration through which a light water (H_2O) electrolyte circulated for 14 days. They also used four analytical techniques, three of which were the same as those used by Mizuno and his colleagues, with Neutron Activation Analyses replacing Electron Probe Microanalysis. Some measurements were made both before and after 14 day runs. That enabled them to determine absolute production rates for various elements.

(3) Little and Puthoff Experiments.

These authors provided the results from their transmutation experiments in a web posting in 1998[16]. They used commercial kit, which contained equipment for experiments very similar to those of Miley and Patterson. The paper described the kit: "RIFEX stands for Reaction In a Film Excited compleX. Clean Energy Technologies, Inc. (CETI) made the RIFEX kit available in late 1996 to provide 'the opportunity to examine and conduct research on CETI's Patterson Power Cell which has received several U.S. Patents and has been acclaimed as the first device to reliably demonstrate chemically assisted nuclear reactions.'" Little and Puthoff ran experiments for 14 days. They used the X-Ray Fluorescence method for elemental analyses. The x-ray energies were limited to the 4-14 keV range, which enabled them to search for 56 elements. A detailed drawing of the cell, and of the overall flow system is provided in their web posting. It is similar to the drawing on the right of Figure 4.

B. Comparisons of Transmutation Data

Six comparisons between four results, the three transmutation data sets and the Optical Model results, can be made. We present a few of them. Overplots and aligned plots are given in the next sub-section. Then, we briefly review a statistical analysis of all four of the results. A discussion of all of the transmutation data follows.

(1) Comparison Plots

As noted already, Little and Puthoff used a setup similar to that of Miley and Patterson. That motivated them to provide a direct comparison of their 1998 results with the 1996 data from Miley and Patterson. Their overplot is shown in Figure 5. In describing the plot, Little and Puthoff wrote "It is immediately apparent that there is a substantial similarity between these results. The SIMS detected scores of elements in our Run 3 beads at levels similar to those found in Miley's runs!" We have added vertical lines to the Little-Puthoff plot at positions of the five peaks in Optical Potential model, which is in Figure 1. It can be seen that the data in both of the experimental runs scatter significantly. However, they tend to be higher near the peaks in the theoretical model.

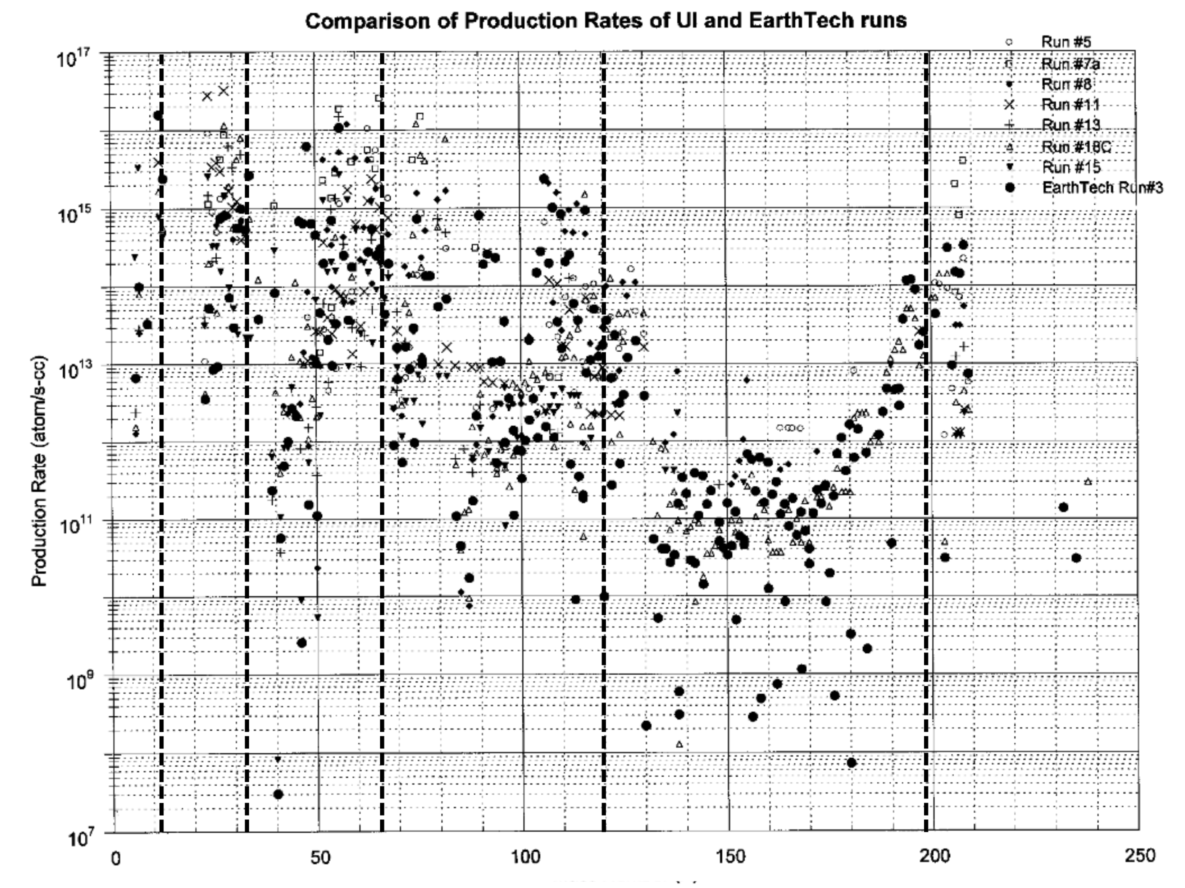

Figure 5. Overplot of the transmutation results from EarthTech run #3 by Little and Puthoff (heavy black dots) with the data from seven runs by Miley and Patterson (other symbols). The vertical dashed lines are at the positions of the peaks in the Optical Model, as shown in Figure 1.

In contrast to the overplot of transmutation results shown in Figure 5, there is no direct comparison of the data from Mizuno with that from Miley and Patterson. Hence, the aligned plot of the two separate data sets shown in Figure 6 was constructed. Again, the graphic contains the five vertical lines at the atomic numbers where the theoretical optical model shows peaks. It is seen that, once more, the scattered data have apparent peaks that align with the model about fitting neutron wavelengths into nuclei of various sizes. It is worth noting again that the Miley and Patterson data in the top of Figure 6 is from before-and-after measurements of elemental concentrations. In contrast, the data from Mizuno and his colleagues is from post-run measurements. Despite that significant difference, both data sets show five peaks at about the same positions, and the peaks align with those in the theoretical neutron-fitting model.

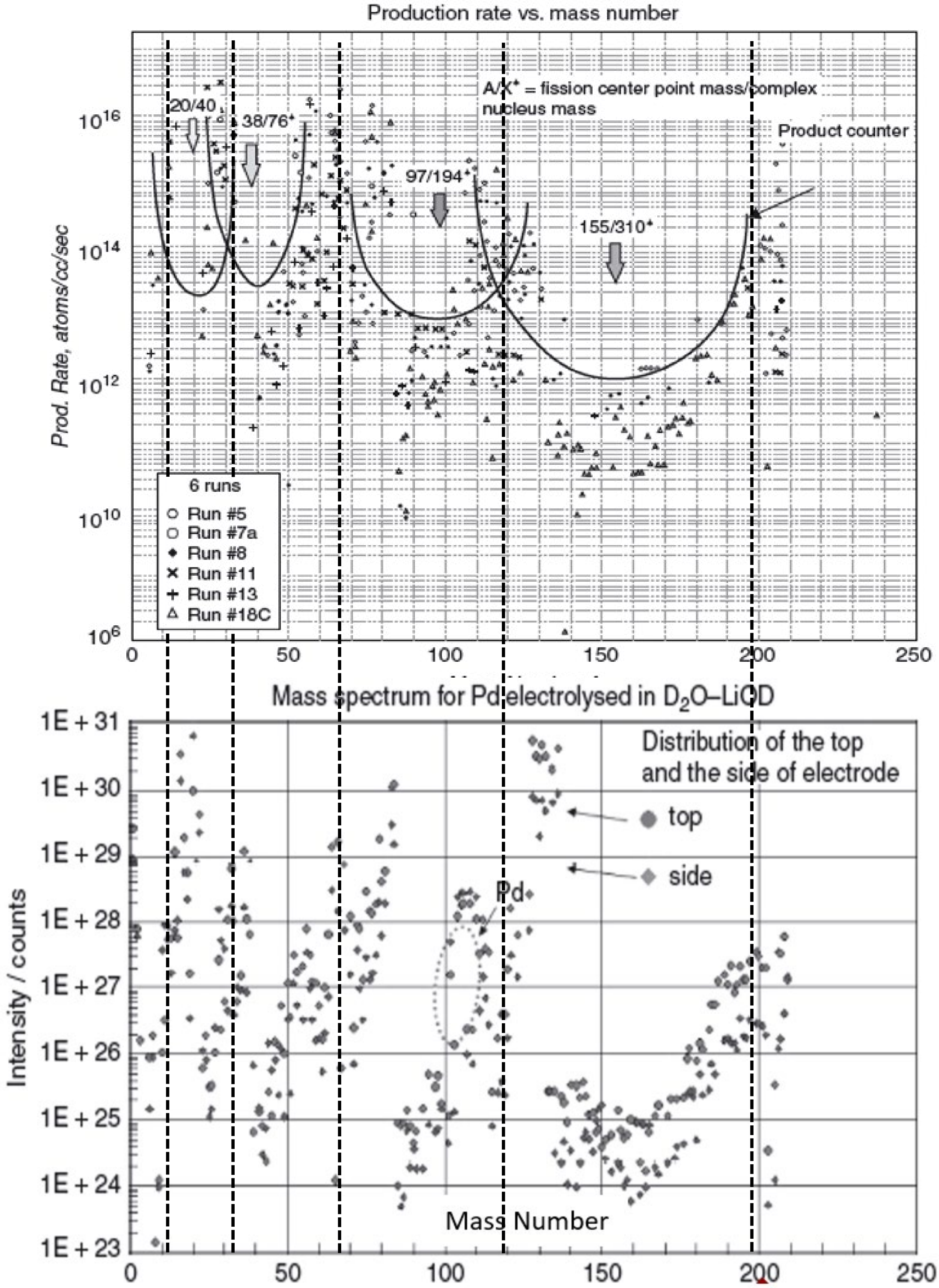

Figure 6. Transmutation data as a function of atomic mass A in AMU. Top: Absolute elemental production rate in atoms per cubic centimeter per second from Miley and Patterson. Bottom: Count rate from mass spectrometry measurements by Mizuno, Ohmori and Enyo. The vertical dashed lines are at atomic mass numbers that are the same as the peaks in Figure 1.

(2) Statistical and Data Analyses

The plots in Figures 5 and 6 indicate correlations between the three transmutation data sets. However, they are qualitative and subjective. It is possible to perform quantitative and objective tests of the correlation of such data sets. Such tests were done by Scholkmann and this author[17]. We also included transmutation data from Yamada and his colleagues[18] in that study. That paper reported increases in concentrations of several elements, specifically Ti, Cr, Mn, Fe, Ni, Cu and Ag, but no peaks as a function of mass. The results of our study are as follows.

> In the present study, we analyzed whether three available nuclear transmutation data sets show a consistent pattern and whether this pattern correlates with a model-based prediction of Widom and Larsen. Our analysis revealed that the data sets exhibit a similar pattern and correlate with the computed function. The last three peaks as a function of atomic mass A (intervals: 64–70, 116–129, 191–208 A*)* were significantly ($p < 0.05$) correlated with the averaged data despite great differences in the experiments.

The three data sets noted in this quotation are those shown in Figure 3:

In some of the later figures in this paper, the quantities of interest are plotted as a function of atomic number Z rather than atomic mass M. The chart of the nuclides[19], and Wikipedia articles on several elements, were used to make the following correspondence between the two measures of the size of atoms:

A	12	32	66	120	198
Z	6	16	30	51	79

The data graphics in Figures 5 and 6 are not the only way to determine the appearance of new elements in LENR experiments. Storms studied many papers that reported the apparent production of new elements, that is, transmutation products. He produced a histogram[20] of the

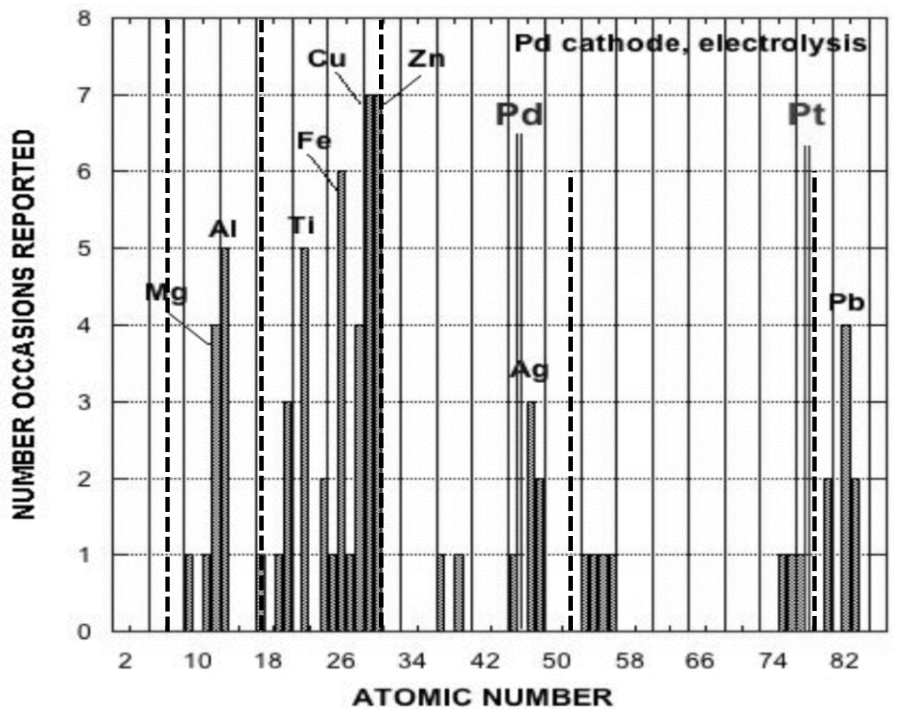

Figure 7. Histogram of the number of published papers and reports that claim the production of specific elements in LENR experiments, as labelled on this plot from Storms. The dashed lines correspond to the values of Z in the table above.

frequency with which various elements were reported, which is shown in Figure 7 as a function of atomic number. The vertical dashed lines in that figure are located at the atomic numbers shown in the table above, which correspond to the atomic masses where the peaks occur in Figure 1. The elements, which were reported most frequently, cluster near a few specific values of atomic number (mass). It is seen that two of the dashed lines, the third and the fifth in order of increasing atomic number, align nicely with peaks in the histogram. The first, second and fourth peaks are near other peaks, but not as well aligned. The comparison is Figure 7 can be taken as suggesting an imperfect alignment of the frequency of reports of elemental production with the more synoptic experiments, the results of which are in Figure 5 and 6. Still, the compilation by Storms tends to corroborate the data from Miley and Mizuno. The basic reason for this behavior, that is, the appearance of peaks for some atomic masses and associated numbers in various types of transmutation data, is not understood, despite an optical model calculation of how neutron wavelengths fit within nuclei of specific sizes[21].

(3) Discussion of Transmutation Data

The transmutation data presented above are quite scattered. However, they are valuable because they represent major milestones in the experimental study of LENR. The research by Miley and Patterson was the first study that spanned almost all of the periodic table. Most earlier studies sought to measure light elements, notably helium, from deuterium fusion and similar reactions between light nuclei. The study by Mizuno and his colleagues, and the later study by Little and Puthoff, had the very significant feature of validating the results obtained by Miley and Patterson in both remarkably different and very similar types of LENR experiments. Such validations did not happen often in the first decade of the study of LENR, especially for complex experiments and analyses.

Importantly, the transmutation data from all three laboratories had five peaks, and all five agreed with each other at similar values of atomic mass. Further, the peaks occur at the same five atomic masses as the well-defined peaks in the optical potential model of neutron absorption computed by Widom and Larsen. Also, Miley and Patterson. observed excess heat, and Mizuno *et al.* measured anomalous isotope ratios. Little and Puthoff sought to measure excess (LENR) heat, but did not find any. The complex and detailed transmutation studies added much to the growing empirical data on the reality and characteristics of LENR. Similar studies with other types of LENR experiments, such as hot gas and plasma loading, would be valuable. Further, searches for radioactivity in the materials after such experiments could be interesting. Measurements of isotope ratios for various elements in the transmutation products would probably be fruitful for understanding which specific nuclear reactions occurred.

The key issue with quantitative understanding of transmutation data is clear. Measurements of elemental production rates depend on four factors, (a) the number (concentrations) of starting atoms of the elements in the experimental materials, (a) the reaction rates for each element (isotope), (c) the duration of experiments, and (d) the sensitivity of the instruments and techniques used for elemental quantification. The amounts of elements at the end of LENR experiments as a function of atomic mass depends on two major distributions, (a) the starting elemental distribution and (b) the distribution of nuclear reaction rates as a function of atomic mass. Knowing only rates is insufficient to understand quantitatively what has been measured in LENR transmutation experiments. Those two distributions could each have been either flat as a function of atomic mass, or else peaked at mass numbers where the empirical peaks were observed. That is, there are four combinations, three of which might have produced the peaks that were observed. If both the starting concentration and rate distributions were flat, peaks would not have been observed.

To further complicate understanding of the transmutation results, there are several nuclear reactions that might have occurred. Most of the literature on LENR deals with the fusion of light nuclei, especially fusion of two deuterons. However, the transmutation data sets imply LENR occur, which involve nuclei with masses across the periodic table. Addition of one neutron to any nucleus would increase the atomic mass A, but not change the atomic number Z or increase the concentration of an element. However, subsequent electron emission could have increased the value of Z by one, increasing the concentration of element Z+1 at the expense of a decreased concentration of element Z. Both mass-increasing reactions with no elemental change, and elemental-change reactions with or without significant mass changes are possible. Importantly, it is not known if any or many of the nuclei in the starting material underwent more than one nuclear reaction during the long experiments. If multiple sequential nuclear reactions were possible and occurred, elements might be depleted where the rates are the highest and accumulate where the rates are lowest. However, that seems to be contrary to the data, and the expectations of Widom and Larsen. Further, the possibility of fission of heavier nuclei leading to their depletion with increases in the concentrations of lighter nuclei has also been discussed[22].

4. Screening in Deuteron Fusion Experiments

The transmutation data reviewed in the last section almost spans the entire periodic table. We now turn to the fusion between two deuterons, one of the lightest of the nuclei. Such fusion has been done using target materials across much of the periodic table. However, the experiments discussed next are very different from the LENR experiments that followed the 1989 announcement by Fleischmann and Pons. Now, we are concerned with classic collision physics experiments in which accelerated ions impact targets with enough energy to overcome the Coulomb barrier and experience nuclear reactions. Such experiments were done at higher and higher collision energies, MeV and even GeV, throughout most of the 20th century, as more capable accelerators were built. However, there was also much interest in collisions at low energies in the keV range, due to the need for data in astrophysics and hot fusion research. That interest began long before 1989. “Cold Fusion”, now LENR, added another reason for doing low-beam-energy experiments. Many such experiments have been motivated by the possibility that they will lead to a fundamental explanation of LENR.

Before starting this section, it is worthwhile to pause to consider the complexity of the structures and process we will review. We are dealing with ions impacting targets. The ions are generally lone nuclei, but can also be molecules, both of which have widely-varying kinetic energies. The targets have compositions and structures, both on and near their surfaces, and in their bulk, which are complex and also vary widely. Since many targets are crystalline, the orientation of the target is also a significant variable. The surface of the target can range from clean, free of any foreign atoms or molecules, to partially or fully covered with atoms or molecules that are physically adsorbed or chemically bonded to the surface. The nanometer-scale structure of surfaces can include anything from near-perfect lattices to highly defective layers. The bulk of materials ranges from single crystals, for example, highly perfect silicon from the semiconductor industry, to polycrystalline structures with grains of diverse shapes and sizes. The interior of materials can contain defects of different dimensions, from 3D (volume) inclusions and voids to 2D (sheet-like) grain or twin boundaries to 1D (linear) edge or screw dislocations, and 0D (point) vacancies or impurity atoms, all in any combinations, distributions, and densities.

All of the diversity just describes deals only with the static characteristics of the target. But obviously, beam impact experiments are highly dynamic. The motions of the incident ions even near and, especially, in a target are highly varied and complex. Multiple scattering is commonplace within solids. The responses of the nuclei, bound electrons, and bonding electrons on the surface and inside of the target are similarly diverse. The rates at which nuclear reactions occur are influenced by all of these factors. However, experiments yield relatively few numbers, not enough for detailed descriptions of all the relevant dynamics. Cross sections and screening potentials are derived from the measured rates. They are valuable in themselves. However, theoretical understanding, that is, quantitative computation of those parameters, requires consideration of some of the complexity of the actual physical situation, as well as many approximations.

Despite the complexity just noted, the essence of screening during nuclear collision experiments can be understood by use of the two schematics in Figure 8. The diagram on the left depicts screening as the projectile nucleus advances continuously from right to left in space toward the target nucleus. When the positive projectile nucleus is distant from the target, it does not feel full repulsion from the target nucleus because the electrons that surround the target nucleus neutralize (screen) the field of the target nucleus. However, when the incoming nucleus penetrates the cloud of electrons around the target nucleus, the outermost electrons bound to the target nucleus no longer provide thorough screening. Then, the two nuclei start to experience mutual repulsion. By the time the nuclei just begin to contact, there is no longer effective screening. The strength of the mutual repulsion of the two positive nuclei at that point is the maximum height of the Coulomb barrier.

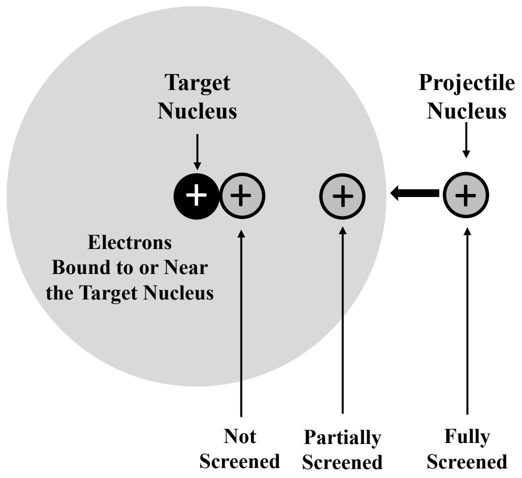

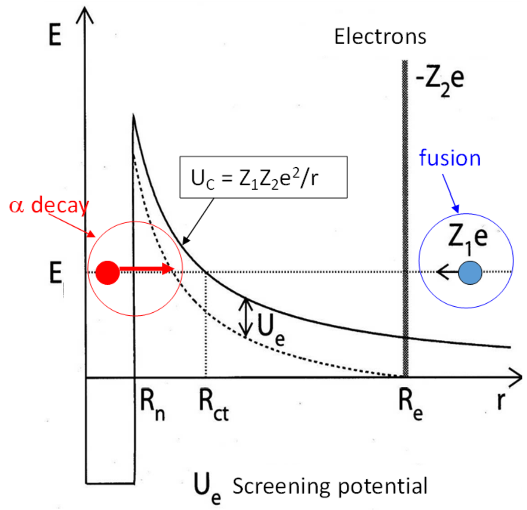

Figure 8. Left: Schematic of the projectile nucleus positions at three times before a nuclear collision. The nuclei are shown as 1/10 of the atomic size. In reality, the nuclei are 1/100,000 the size of an atom. Right: Schematic by Kasagi of the kinetic and potential energies for (a) an incident projectile with charge Z_1e (blue) and (b) an alpha particle escaping from a radioactive or other nucleus (red).

The diagram on the right in Figure 8 shown the energetics during that collision process[23]. In the absence of screening, the incoming particle with energy E_l encounters the Coulomb potential barrier, $U_C = Z_1Z_2e^2/r$, where r is the separation between the two nuclei. The projectile has to tunnel from the distance R_{ct} to reach (contact) the target nucleus in the deep Yukawa potential well that is due to the strong force. Screening due to electrons from around the distance of R_e, lowers the Coulomb potential barrier by U_e, shortening the tunneling distance and increasing the nuclear reaction rate. Figure 8 also shows the energetics for alpha decay from a radioactive nucleus. Historically, it was considered by Gamow long before screening effects on nuclear reactions. Both processes depend on the tunneling probabilities, collisions from the outside and alpha particle emission from the inside.

Screening has a major effect on collisions at low beam energies. This can be illustrated both mathematically and from measured data, as in the following paragraphs.

The equation for the nuclear reaction cross section without screening is:

$$\sigma(E) = [S(E)/E] \times \exp(-2\pi\eta) = [S(E)/E] \times \exp[-(E_g/E)^{0.5}].$$

With the screening potential U, such that U << E, the equation becomes:

$$\sigma(E) = [S(E)/\{E(E + U)\}^{0.5}] \times \exp[-\{E_g/(E + U)\}^{0.5}].$$

S(E) is the Astrophysical Factor. It is introduced to take into account the rapid variation of cross sections with energy E, which is due to the Coulomb repulsion between the positive nuclei. Use of the Astrophysical Factor makes more accurate the extrapolation of cross sections measured at higher beam energies to the lower kinetic energies in plasmas of astrophysical and hot fusion interest. The parameter $\eta = Z_pZ_te^2/4\pi\varepsilon_oV$, where the Z are the atomic numbers of the projectile and target, e is the electron charge, and ε_o is the dielectric constant of free space.

The probability of overcoming the Coulomb repulsion by tunnelling through the Coulomb barrier into a nucleus is given by the Gamow Factor = $\exp[-(E_g/E)^{0.5}]$, where the Gamow Energy is $E_g = 2\, M_R\, (\pi\alpha Z_pZ_t)$. The factor α is the Fine Structure Constant ~ 1/137. M_R is the reduced mass in the center-of-mass reference frame. $M_R = m_pm_t/(m_p + m_t)$, where the m values are the masses of the interacting projectile and target nuclei[24]. That reference frame is a coordinate system for colliding particles in which the center-of-mass remains at the origin of the coordinate system prior to the collision[25]. Use of the center-of-mass reference frame simplifies the equations describing the kinematics of a collision between particles.

It is possible to form a ratio of the enhanced cross sections with screening to the cross sections without screening. The resulting Enhancement Factor, denoted F, explicitly exhibits the effect of screening as a function of the collision energy. The result is $F = \exp[\pi\eta\,(U/E)]$, where E is the center-of-mass energy and the screening potential U<<E. This shows that the effect of screening becomes exponentially more important as the center-of-mass (and beam) energy decreases. Note that the Enhancement Factor does not depend on the density of target atoms or the rate at which the projectile decreases velocity as it loses energy to the target. It depends on the screening constant, which depends on the electron density in the target. Examples of measured Enhancement Factors are given below in Figure 6.

The energies for which it is necessary to consider enhancement due to screening have been noted[26]: "For energy ratios E/U > 1000, shielding effects are negligible, and laboratory experiments can be regarded as essentially measuring $\sigma_{BARE}(E)$. That is true even though the target nuclei are inside of solids. However, for E/U < 100, shielding effects cannot be neglected and become important for understanding low-energy data." The experiments of interest here generally have E in the range of 1000 to 10,000 eV and U values smaller than 1000 eV, commonly about 100 eV. That is, E/U is in the range from about 1 to 100.

There are two types of plots for screening data in D-D fusion reactions that are common and valuable. An example of the first is shown in Figure 9[27]. The top of that figure shows the thick target yield as a function of the deuteron impact energy in the range from 10 keV down to a few keV. The rapid decline in the deuteron fusion rates as the beam energy is decreased is evident. That decline is what makes experiments at low beam energies challenging. Long runs are needed to obtain adequate statistics for precise measurements. The measurements fall

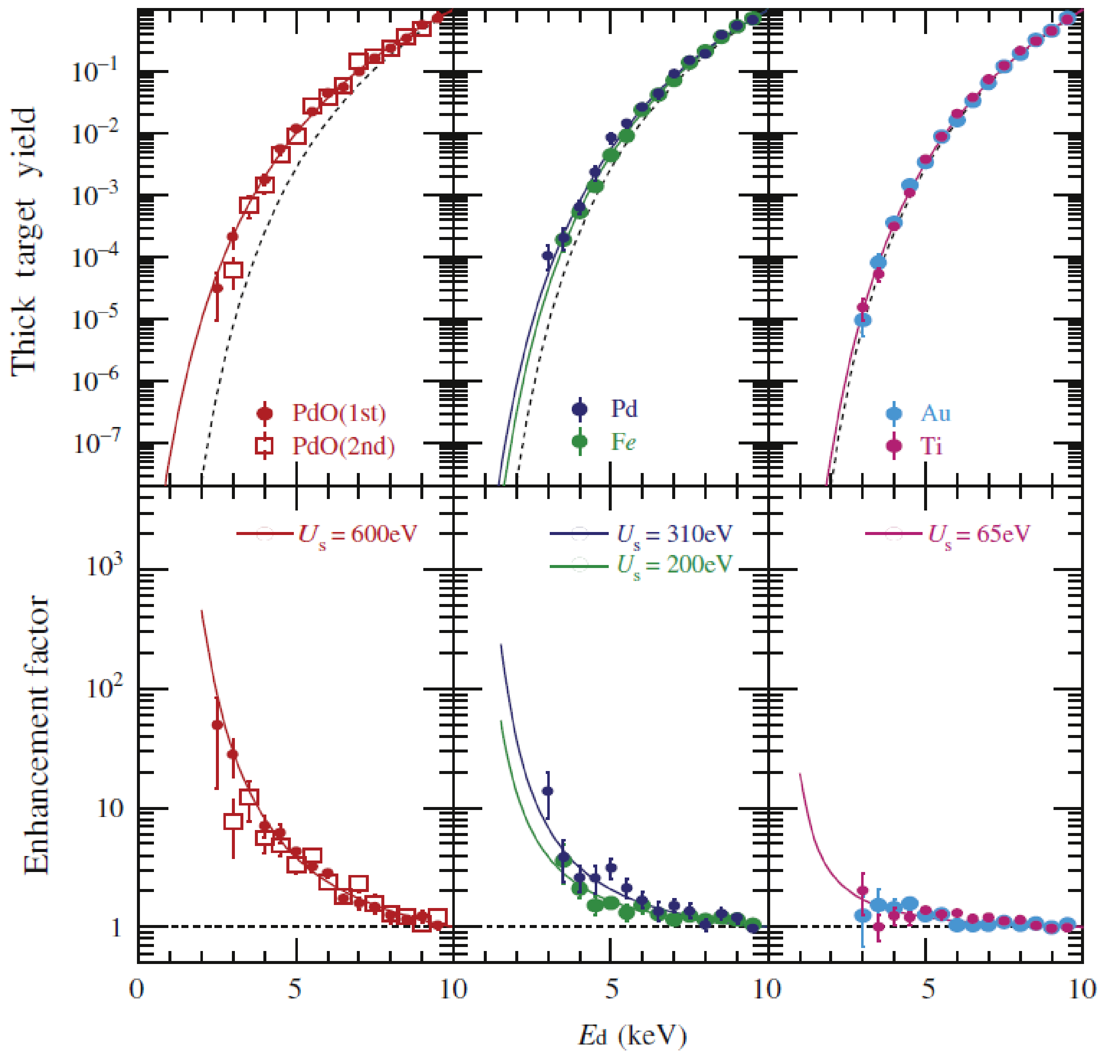

Figure 9. Top: Thick target fusion reaction yields for five different targets bombarded with deuterons at the indicated energies below 10 keV. The yields are normalized to unity at 10 keV. The dashed lines are extrapolations of the curves for higher impact energies. Bottom: Ratios of the measured and extrapolated yield values, with computed ratios for different screening potentials noted in the figure (solid lines).

significantly above the values expected from extrapolation of the yields obtained at higher bombarding energies. The latter are shown by the dashed lines in Figure 9. The ratios of the measured yields to the extrapolated yields, the Enhancement Factors, are shown in the bottom of the Figure 9. Those curves can be fit by assuming various values for the screening potentials, as indicated. That is one way in which numerical values for the screening potentials can be obtained from measured data.

5. Compilations and Comparisons of Screening Potentials

The second type of plot for screening potentials shows empirical values of those energies as a function of the atomic number of the targets in which deuteron fusion reactions occur. Two versions of that kind of plot are in Figure 10. An early graphical summary of screening potentials for targets across the periodic table was provided as Figure 3 in a 2006 paper by Czerski and his group[28], and later as Figure 11 in a 2008 paper by Huke and Czerski's group[29]. That graphic is reproduced in the top of Figure 10. It should be noted that there are about 100 experimental screening potentials in the Czerski graphic. That reflects the interest in the topic

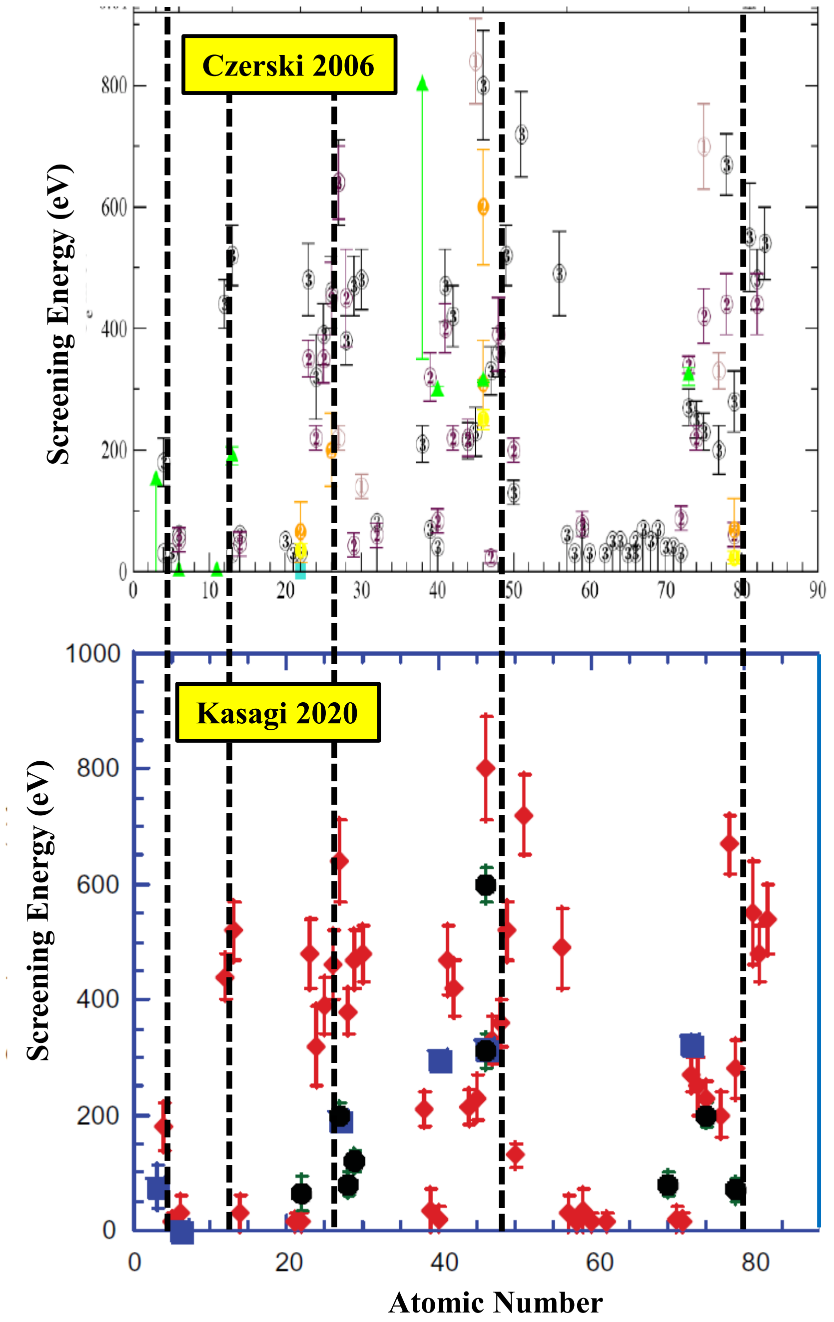

Figure 10. Compilations of empirical screening potentials for deuteron fusion as a function of the atomic number of the target material in which they were measured. The five dashed lines are at the same values of atomic size as in the earlier plots.

of screening potentials for fusion reactions. The data from the active laboratories scattered widely. However, it is possible to discern regions of high potentials and regions of low potentials. The "peaks" are qualitatively similar to those in the transmutation data sets, not entirely clear but still suggestive. A later compilation by Kasagi in 2020 also shows potential peaks despite similar scatter in the data[30]. Figure 10 has Kasagi's plot at the bottom.

The comparisons above are between measured screening data. However, there are also plots of theoretical screening values across the periodic table. We pause to note two differences between theoretical and empirical screening data sets. That is done by the use of Figure 11 from Huke, Czerski and their colleagues[28]. It shows both measured and computed screening

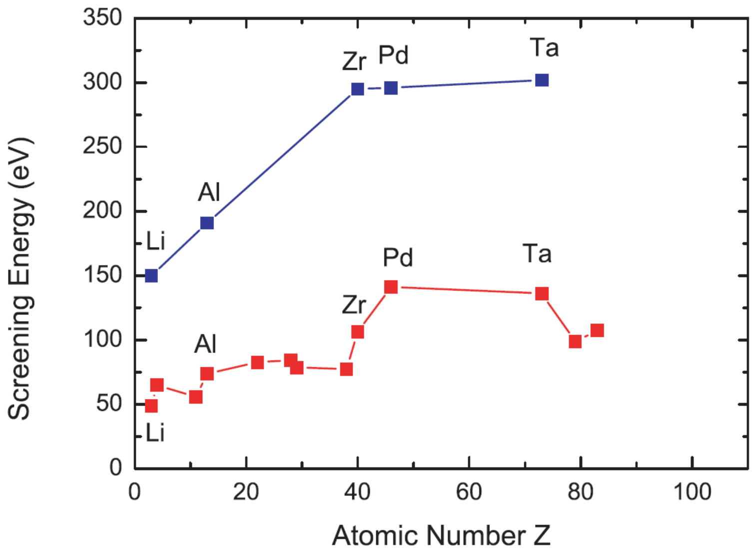

Figure 11. Screening potentials as a function of atomic number z. Top in blue: empirical values. Bottom in red: theoretical values.

potentials across much of the periodic table. The differences in magnitude of roughly a factor of two are unexplained. The trend is for both screening potentials to increase with atomic number, save for the potentials computed for the heaviest elements. There is no indication of the peaking that is perceived in Figure 11. If the idea in this paper that such peaks do occur withstands scrutiny, the theories for screening energies will need modification.

6. Correlation of the Transmutation and Screening Data Sets.

The vertical dashed lines in Figure 10 are at the atomic numbers corresponding to the peaks in the optical potential model calculations of Widom and Larsen (Figure 1) and the transmutation data sets of Miley and Mizuno (Figure 3). That is, compilations of electron screening potentials from deuteron fusion experiments at low beam energies by Czerski and Kasagi have peaks that align with peaks in the theoretical and transmutation data.

The alignments of the peak locations between the transmutation and screening data sets are imperfect. Nonetheless, there are clear regions of both high and low screening potentials, and the number of regions of high values appears to be five, the same number as in the theoretical and transmutation data. Those similarities motivate consideration of the potential implications of the peaking of both transmutation and beam fusion data at roughly similar values of atomic mass. Is there some mechanism in common, which is active in producing both data sets, despite the very different nature of the LENR experiments?

7. Potential Correlations with Other Data

Before discussing aspects of theory for the observations reviewed above, we pause to look for other correlations with data sets across the periodic table from nuclear experiments. Two topics, nucleosynthesis and muon capture, are summarized in the following paragraphs.

A. Natural Elemental Abundances

A paper on genesis of heavy elements was already noted at the end of Section 2. It contains three plots of different nuclear abundances as a function of atomic number or mass across the periodic table. There are peaks in some of the plots, a few of which align with one or two of the peaks discussed in this paper. However, no overall correlations are apparent.

The transmutation data in Figure 6 raised a question about both the Miley and Mizuno data sets being artefactual, due only to terrestrial or other contaminations. Hence, Scholkmann and this author did a statistical study to examine the relationships of those two data sets with the abundance of nuclei in the earth's crust[31]. The abstract of that paper summarizes what was done and found:

> We showed in a previous study that (i) the transmutation data of three independent experiments have a similar pattern and (ii) this pattern correlates with a model based on the prediction of Widom and Larsen (WL). In the present study, we extended our analysis and investigated whether the abundance of elements in Earth's crust is correlated with either the WL prediction, or the three LENR transmutation data sets. The first analysis revealed that there is no statistically significant correlation between these variables. The second analysis showed a significant correlation, but the correlation only reflects the trend of the data and not the peak-like pattern. This result strengthens the interpretation that the observed peak-like pattern in the transmutation data sets does not originate from contamination.

The paper went on to discuss two possible concerns about transmutation data, which could not be eliminated by the statistical analyses. Both were highly unlikely. Overall, that 2016 paper supports the idea that the transmutation data of Miley and Mizuno are due to nuclear reactions in their experiments, and not due to laboratory and experimental contamination.

The report by Little and Puthoff on the internet contained a cautionary statement about contaminations from within their RIFEX experiment: "We believe that these elements appear in the reacted beads as a result of electrodeposition of cations in the electrolyte that were either present initially or were dissolved from various sources in the electrolyte circuit." They were referring to the elements Fe, Zn and Pb. It seems clear that additional transmutation experiments are needed, with great care to avoid any sources of contamination. However, the alignment of the five peaks in the transmutation data sets with peaks in screening data and the Optical Model theoretical calculations support the possibility that contamination is not a dominant problem in the transmutation experiments.

B. Muon Capture Data

Another broad nuclear data set came to our attention, which is very different from those discussed above. It involves the capture of muons by atoms. Muons are leptons, as are electrons, but are 207 times more massive than electrons[32]. They have a lifetime of 2.2 μs, but that is time for them to be captured in atomic orbitals[33]. Once captured in atomic orbitals, muons can either decay, or be captured by a proton of the nucleus, producing a neutron and neutrino, and sometimes gamma-rays or charged particles[34]. Hence, muon capture by nuclei is a two-step process, the first being atomic and the second nuclear.

Unlike the various plots of nuclear abundances in Nature, maxima in the muon capture data align quite well with the peaks in transmutation and screening data discussed in this paper. Figure 12 shows the capture rates in comparison to the locations of the peaks in transmutation and screening data. The graphic in the top of the figure is from a 1977 review of muonic capture[35]. The data in that graphic came from a 1966 paper by Zinov *et al*[36]. The caption of Figure 12 contains a quotation from the paper from which the figure was taken. The following slightly-edited quotation from the paper explains the figure:

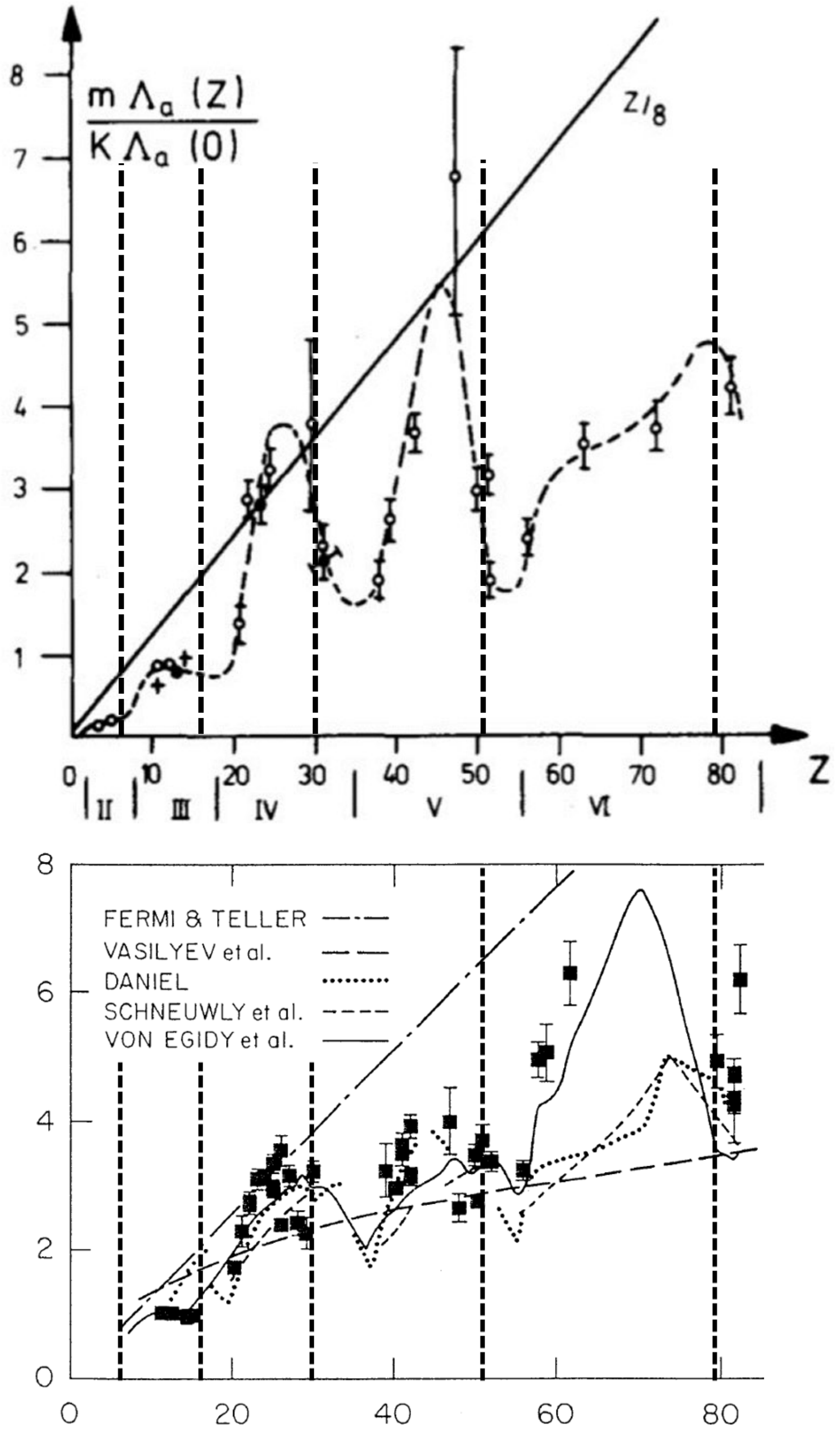

Figure 12. Top: "Periodicity of the relative atomic capture probability $m\Lambda_a(Z)/K\Lambda_a(0)$ in metallic oxides Z_KO_m. Numerals II……VI represent the groups in the periodic table to which the metallic atoms belong." The expectation of the Fermi-Teller law is represented by the straight line. Experimental data are from Zinov *et al.* Bottom: "Comparison of experimental and theoretical atomic capture ratios in oxides. The data are those of Stanislaus *et al.* The Fermi–Teller Z law is clearly inadequate as is the monotonic form of Vasilyev. Atomic structure is included in the calculations by Daniel, Schneuwly *et al.*, and von Egidy *et al.*, the theory with the best fit." The vertical dashed lines in both plots occur at the same elements as in the earlier figures.

Fermi and Teller, by simple arguments and the assumption that the atomic capture probability of a muon is proportional to the energy loss of the muon near the atomic species constituting a compound or a gaseous mixture, concluded that the atomic capture rate Λ_a is given by the proportionality relation $\Lambda_a \sim Z$, Z being the nuclear charge of the atom stopping the muon. This so-called "Z law" implies that, for a binary compound A_nB_m, the ratio of atomic capture rates for the constituting species will be given by $\Lambda_a(A)/ \Lambda_a(B) = [nZ_A/[mZ_B]$. Experiments done in the last decade indicate that there is no such simple law as that relation valid for all compounds. Deviations from the Fermi-Teller law have been carefully studied, and are found to be generally associated with the effects of atomic shell-structure and chemical environment.

It is noted that the alignment of the peaks in the muon capture data in the top of Figure 12 is imperfect. The fifth peak appears to be well aligned. The fourth and third peaks fall to the left of the atomic numbers for the transmutation and screening data. However, the dashed lines could be redrawn to make the matches look better. The second and first peaks are not strongly defined, and appear to fall below the two dashed lines at the lowest atomic numbers. In general, the alignments between the transmutation and screening data are better than between those two data sets and the muon capture data.

The data in the plot in the bottom of Figure12 is from a 2001 review of muon capture in oxides[37]. Included are data from a 1987 experimental paper[38], and lines from five theories. Two of the theories predict monotonic increases in the muon capture probabilities as a function of atomic number, which disagree with the data. Three of the theories include details of atomic structure, which give improved agreement with the measurement. The data and three theories in the bottom of Figure 12 show indications of peaks. The two near Z = 30 and 51 are close to the third and fourth peaks in the transmutation and screening data. However, there is little alignment with the other three peaks in Figures 6 and 10.

Why the peaks in that muon capture data should align as well as they do with those in the transmutation and screening data is another mystery. The production of a neutron during muon captures might play a role in explaining the alignment. The alignments shown in Figure 12 could be the focus of another study. The central question is whether the approximate alignments have a fundamental explanation, or else are only accidental.

8. Discussion.

We comment on some of the points made in this paper, and on other related topics. Then, we provide a perspective on the potential use of Artificial Intelligence (AI) to discern connections between data sets, such as those discussed above.

A. Nuclear Topics

The concept of fitting integral numbers of wavelengths of neutrons within nuclei into the diameters of specific nuclei is central to the Widom-Larsen optical model calculations. Given the empirical relationships to the transmutation and screening data, the idea is also important for understanding the apparent peaks in those two types of LENR data. One issue relative to that "resonance" concept is non-uniform distributions of nucleons within nuclei, so-called neutron skins. A 2022 paper entitled "Ab initio predictions link the neutron skin of ^{208}Pb to nuclear forces" began by noting "Heavy atomic nuclei have an excess of neutrons over protons, which leads to the formation of a neutron skin whose thickness is sensitive to details of the nuclear force." The neutron skin thickness in ^{208}Pb was computed to be 0.14 to 0.20 femtometers. That is small compared to the diameter of the ^{208}Pb nucleus, which is 7.11 fm. Hence, the idea of fitting neutron wavelength into nuclei to explain the positions of the peaks in the transmutation and screening data seems viable. Further, it is noted that the alignment of the screening potential data in Figure 10 with the transmutation data is quite good for the lowest mass nuclei, for which the neutron skin depth might be the least.

Nuclear reactions, including LENR, are dynamic. So, it is reasonable to consider the dynamics of the interactions that lead to transmutations on or in solids, and collisions that cause fusion reactions at low beam energies in targets. In the case of the beam experiments, a relatively slow incoming deuteron might be oriented such that the neutron within the deuteron first encounters a target nucleus. That orientation could be due to the long-range electrostatic repulsion of the proton in the deuteron by the target nucleus. If there were such an orientation, then the fitting of a neutron into the target nucleus might be significant, leading to peaks at the atomic masses and numbers seen in the screening data. While speculative, such dynamics are conceptually simpler than the situation for transmutations on or within solids. The high density of atoms within solids would lead to significant multiple scattering, making less likely the possible orientation of deuterons such that their neutrons first encounter reaction partners. However, maybe there is time during both beam experiments and during LENR on and in materials for the proton in the deuteron to move into a position "behind" the neutron.

Deuteron stripping has come into the discussion of LENR mechanism a few times. In a stripping reaction, part of the incident nucleus combines with the target nucleus, and the remainder of the incident nucleus proceeds with most of its original momentum in almost its original direction[39]. During a deuteron stripping reaction, the incident neutron stays in the target, attracted by the strong force, and the proton never enters the target nucleus, due to electrostatic repulsion. Such reactions have commonly been used to study both nuclear structure and reactions. A 1958 paper[40] was entitled "The Study of Nuclear Collective Motion by Stripping Reactions". The topic is much older. A review[41] of stripping reactions traces the origins of the topic to a 1935 paper by Oppenheimer and Phillips[42]. The first book on stripping reactions was published in 1957[43]. This author wrote a review of deuteron stripping reactions in 1966 with 32 references[44]. A 2020 review of the theory of deuteron stripping reactions[45] has already been cited over two dozen times. The goals of that paper are stated, as follows:

> Here we offer a comprehensive review of recent progress made with these theories, with the aim of familiarizing experimentalists with new theoretical developments and thus eventually improving the quality of spectroscopic and other nuclear structure information extracted from experiments. Another aim of this review is to provide a guide for nuclear structure theorists working to extend the application of nuclear structure theories to nuclear reactions, especially in the context of *ab-initio* calculations. *Ab-initio* approaches to the description of many-body systems are booming in all areas of physics and chemistry due to significant improvements in computing power and huge progress in high-performance computing.

It remains to be seen if any of the theoretical methods cited in that review will turn out to be relevant to simulating and understanding LENR.

There are three theoretical papers in the literature on LENR that involve deuteron stripping reactions. The first, published by Passell in 2015, is intitled "The Case for Deuteron Stripping with Metal Nuclei as the Source of the Fleischmann–Pons Excess Heat Effect"[46]. The author examined data from several LENR experiments that might be consistent with the idea that deuteron stripping reactions are the basis of LENR. He discussed a potential mechanism for the occurrence of such reactions. The paper concludes with the statements "A large advantage of the deuteron stripping hypothesis is the lack of ambiguity over the mechanism for conversion of energy from excited nuclei to heat. Heating by fast protons stopping in matter is a well-established heating phenomena."

In a 2016 paper, Davidson discussed variable mass nuclear particles[47]. His abstract reads as:

> A recent and somewhat radical theoretical explanation for LENR is reviewed. It is based on variable mass theories of relativistic quantum mechanics that date back to the 1930s in works by Fock and Stueckelberg, and up to the present by many others. It explains a large number of observed anomalous effects in LENR by positing that nuclear rest-masses can vary in "nuclear active environments" in condensed matter settings. The varying masses modify the kinematic constraints of the nuclear reactions. It also offers a mechanism for enhancing electron screening and-or quantum tunnelling rates, for allowing for resonant tunnelling, and for modified radioactive decay rates by mass changes in the decaying isotopes.

That paper includes the following comments on diverse nuclear reactions, including deuteron stripping reactions:

> With varying particle masses, transmutations can in theory at least occur in a number of ways in nuclear active environments. Enhanced electron screening caused by electron mass increases can modify alpha decays, beta decays, and electron capture rates. Mass changes of nuclei can change reaction rates or make reactions possible which would normally be forbidden. Resonant fusion of hydrogen or deuterium with other nuclei, resonant fusion of alpha particles and other nuclei, and even fission of heavier nuclei might occur after a mass change. Also, there is the possibility of neutron creation and subsequent capture as in the Widom–Larsen theory, or neutron stripping or hopping reactions, leading to many possible transmutations. In short, a world of possibilities exists, and a menagerie of transmutations have already been observed experimentally in LENR

Li and his colleagues published another theoretical paper on LENR in 2019, which involved stripping reactions[48]. Part of the abstract of the paper follows:

> A resonant surface capture model is proposed to explain the various phenomena: the temperature dependence of excess heat, nuclear fusion cross-section data from beam–target experiments and from condensed matter nuclear reactions. This model is based on Oppenheimer's stripping nuclear reaction, and Bethe's solar energy calculation using the resonance effect to put the incoming projectile at the edge of target nucleus without forming compound nucleus.

The introduction of the paper contains the following overview of the contemplated mechanism:

> This phenomenon reveals an important role of the nuclear resonance. During the elastic process, the resonance would be fully developed without any damping; then, the resonance would put the peak of the wave function at the edge between the nuclear potential well and the Coulomb barrier. The peak implies that the nucleon in the target nucleus would have a chance to directly interact with the nucleon in the projectile, because the nucleons are sticking together and inside the range of nuclear interaction due to resonance. This is a surface capture process that occurs without forming a compound nucleus. The reaction energy would be carried away by the charged nuclear products, and be transferred to the surrounding electrons as excess heat. Thus, an inelastic nuclear scattering process follows an elastic nuclear scattering due to the resonance.

Overall, the possible role of stripping reactions in LENR is still an open question. Modern theoretical tools for the study of deuteron stripping reactions might be examined for their possible applicability to LENR.

B. Artificial Intelligence for LENR Research

The correlations in this paper within both transmutation and fusion screening data sets, and between them, were recognized by the author for two related reasons. First, he heard presentations on most of the referenced data at conferences. Second, he studied the papers that followed the presentations. Individual knowledge of the extensive literature on LENR, over 5000 papers and reports, is the classic way to make connections between the results of various experiments, even if they seem to be unconnected, as in the current case.

In the recent past, another path to recognitions of connections, and even correlations within data sets, has become more widely available. Modern programs in Artificial Intelligence, including Machine Learning and Natural Language Processing, have enabled computer searches for relationships for many years. Use of those tools has been largely restricted to specialists in Computer Science. However, developments in AI during the last few months have made it possible for many others to use AI tools for scientific research and communication.

One new AI program, which became publicly available late in 2022, has received a great deal of attention. It is ChatGPT, a product of the company Open AI. The letters GPT stand for Generative, Pre-trained and Transformer. ChatGPT programs generate responses to prompts by using internal features that were trained on massive data sets, sometimes with human tuning. The word Transformer refers to a type of program, which enables the performance and speed of the new AI programs. The key recent advance in the capabilities of AI programs, including the architecture and functions of Transformer programs, was developed by Google scientists in 2017. It is described in a paper posted on the ArXiv server[49].

At the time of this writing, Chat GPT has been available for just over six months. Rothwell is already a leader in the use of AI for LENR research. He added a version of ChatGPT to the large LENR library of his website lenr.org[50]. He has been posting the results of various tests of the combination on a private CMNS GoogleGroup and on the LENR-Forum[51].

It can be asked if the relationships noted in this paper might be discovered by use of an AI program, such as ChatGPT. That test ought to be done. The software might discover both the relationships of the Miley and Mizuno transmutation data sets to each other, and their connection to the fusion screening data. However, such a success is not assured for multiple reasons. The version of ChatGPT would have to have been trained on data sets including the Miley and Mizuno papers, and also the screening papers. Further, the two transmutation data sets are not closely connected, and they are even more distant from the screening data. Peaks in the screening data, discussed above for the first time, are not in the literature on low-beam-energy fusion experiments. So, the recognized connection discussed in this paper might not be found by an AI program. In the future, when AI programs are able to examine data in plots within papers, they might be able to recognize features between papers that even the authors of the individual papers did not see.

9. Conclusion

The key insights in this work are (a) the apparent five peaks in the compilation plots of screening data from deuteron fusion experiments and (b) the alignment of those peaks with the five peaks in the transmutation data from Miley, Mizuno, and Storms' compilation, as well as the Widom-Larsen theoretical calculations.

The title of this paper begins with the word "potential" because the discussed correlations, while quite apparent, have not yet been established with a detailed and quantitative statistical study. We noted that such a study was done by Scholkmann[17] for the combination of the Widom-Larsen theory, and the transmutation data sets. That study could now be extended to include the screening data compilations from the groups led by Czerski and Kasagi.

This paper deals with four unsolved riddles regarding LENR and other data: (a) what causes the apparent peaks in the transmutation data sets, (b) what causes the apparent peaks in the fusion screening data, (c) why do five peaks occur in both data sets, and align with each other, and (d) is the peaking in the muon capture data related in any way to the peaks in the LENR transmutation and screening data? It could turn out that solutions to these riddles will help with a basic understanding of LENR. In any event, the observations might challenge development of an understanding of the basic mechanisms that enable the occurrence of LENR.

---

[1] A. Widom and L. Larsen, "Ultra Low Momentum Neutron Catalyzed Nuclear Reactions on Metallic Hydride Surfaces", arXiv:cond-mat/0505026 v1 2 May 2005 and European Physics Journal C, vol. 46, pp. 107–111 (2006) DOI 10.1140/epjc/s2006-02479-8

[2] A. Widom and L. Larsen, "Theoretical Standard Model Rates of Proton to Neutron Conversions Near Metallic Hydride Surfaces", arXiv:nucl-th/0608059v2 25 Sep 2007

[3] P. L. Hagelstein1and I. U. Chaudhary, "Electron mass shift in nonthermal systems", arXiv:0801.3810v1 [quant-ph] 24 Jan 2008

[4] V. Vysotskii, "On Problems of Widom–Larsen Theory Applicability to Analysis and Explanation of Rossi Experiments", J. Condensed Matter Nuclear Science, vol. 13, pp. 615–623 (2014)

[5] A. Widom, Y. N. Srivastava, and L. Larsen, "Errors in the Quantum Electrodynamic Mass Analysis of Hagelstein and Chaudhary", arXiv:0802.0466v2 [quant-ph] 5 Feb 2008

[6] Y. N. Srivastava, A. Widom, and L. Larsen, "A Primer for Electro-Weak Induced Low Energy Nuclear Reactions" arXiv:0810.0159v1 [nucl-th] 1 Oct 2008

[7] Y. N. Srivastava, A. Widom, and L. Larsen, "A Primer for Electro-Weak Induced Low Energy Nuclear Reactions", Pramana, vol. 75(4), pp. 617-637 (2010)

[8] L. Larsen, https://www.slideshare.net/lewisglarsen/lattice-energy-llc-hyperlinked-index-to-documents-re-widomlarsen-theory-and-lenrs-september-7-2015. Those graphics are one of 152 such sets that Larsen posted over the years. See: https://www.slideshare.net/lewisglarsen/presentations/3

[9] L. Larsen, "LENRs enable green radiation-free nuclear power and propulsion", https://www.slideshare.net/lewisglarsen/lattice-energy-llc-lenrs-enable-green-radiationfree-nuclear-power-and-propulsion-may-16-2019

[10] https://news.newenergytimes.net/2019/10/31/lenr-theorist-lewis-larsen-dies/

[11] A. Widom and L. Larsen, "Nuclear Abundances in Metallic Hydride Electrodes of Electrolytic Chemical Cells", arXiv:cond-mat/0602472 v1 20 Feb 2006
[12] https://chem.libretexts.org/Courses/University_of_British_Columbia/CHEM_100%3A_Foundations_of_Chemistry/04%3A_Atoms_and_Elements/4.4%3A_The_Properties_of_Protons_Neutrons_and_Electrons
[13] C. Sneden and J. J. Cowan, "Genesis of the Heaviest Elements in the Milky Way Galaxy", Science, vol. 299, pp. 70-75 (2003).
[14] T. Mizuno, T. Ohmori, and M. Enyo, "Isotopic Changes of the Reaction Products Induced by Cathodic Electrolysis in Pd", Journal of New Energy, vol. 1(3): pp. 31-45 (1996) and T. Mizuno, "Isotopic Changes of Elements Caused by Various Conditions of Electrolysis", 237th ACS National Meeting, Salt Lake City, UT (2009).
[15] G. H. Miley, "Possible evidence of anomalous energy effects in H/D-loaded solids – Low energy nuclear reactions (LENR), Journal of New Energy, Vol 2(3-4), pp. 6-13 (1997) and G. H. Miley and J.A. Patterson, "Nuclear transmutations in Thin-Film Nickel Coatings Undergoing Electrolysis", Journal of New Energy, Vol 1 (3): pp. 5-13 (1996) and G. H. Miley "On the Reaction Product and Heat Correlation for LENRs", Proc. of 8th International Conference on Cold Fusion, F. Scaramuzzi (Editor), Lerici (La Spezia), Italy, pp. 419-424 (2000).
[16] S. Little and H.E. Puthoff, Search for evidence of nuclear transmutations in the CETI RIFEX Kit. http://www.earthtech.org/experiments/rifex/rifex.pdf (1998)
[17] F. Scholkmann and D. J. Nagel, "Statistical Analysis of Transmutation Data from Low-Energy Nuclear Reaction Experiments and Comparison with a Model-based Prediction of Widom and Larsen", Journal of Condensed Matter Nuclear Science, vol. 13, pp. 485-494 (2014).
[18] H. Yamada *et al.*, Production of Ba and several anomalous elements in Pd under light water electrolysis. in X. Z. Li (Editor), Condensed Matter Nuclear Science, Proceedings of ICCF-9, pp. 420-426, Beijing, China (2002)
[19] https://www-nds.iaea.org/relnsd/vcharthtml/VChartHTML.html
[20] E. Storms, "Status of cold fusion (2010)", Naturwissenschaften, vol. 97, pp. 861–881 (2010). https://doi.org/10.1007/s00114-010-0711-x
[21] E. Storms, "The Science of Low Energy Nuclear Reaction", p. 96, World Scientific (2007).
[22] I. Savvatimova, Y. Kucherov, and A.B. Karabut. "Cathode Material Change after Deuterium Glow Discharge Experiments" in Proceedings: Fourth International Conference on Cold Fusion Volume 3, TR-104188-V3, pp. 16-1 through 16-11, Lahaina, Maui, Electric Power Research Institute (1993)
[23] J. Kasagi, "Dynamical screening effect on α-decay in metal during deuteron beam bombardment", in Proceedings of ICCF-16 (2011)
[24] https://en.wikipedia.org/wiki/Reduced_mass
[25] https://en.wikipedia.org/wiki/Center-of-momentum_frame
[26] S. Engstler *et al.,* "Isotopic dependence of electron screening in fusion reactions*, Z. Phys. A - Hadrons and Nuclei, vol. 342, pp. 471-482 (1992)
[27] J. Kasagi *et al.*, "Strongly Enhanced DD Fusion Reaction in Metals Observed for keV D+ Bombardment", Journal of the Physical Society of Japan, vol. 71(12), pp. 2881-2885 DOI: 10.1143/JPSJ.71.2881
[28] K. Czerski *et al.*, "Experimental and theoretical screening energies for the $^{2}H(d,p)^{3}H$ reaction in metallic environments", European Physics Journal, vol. A **27**, s01, pp. 83–88 (2006)
[29] A. Huke *et al.*, "Enhancement of deuteron-fusion reactions in metals and experimental implications", Physical Review C, vol. 78, p. 015803 (2008)
[30] J. Kasagi *et al.*, "Screening Energy for Low Energy Nuclear Reactions in Condensed Matter" in J.-P. Biberian (Editor), "Cold Fusion: Advances in Condensed Matter Nuclear Science", Elsevier, pp. 167-187 (2020)
[31] F. Scholkmann and D. J. Nagel, "Is the Abundance of Elements in Earth's Crust Correlated with LENR Transmutation Rates?", Journal of Condensed Matter Nuclear Science, vol. 19, pp. 281–286 (2016).
[32] https://en.wikipedia.org/wiki/Muon
[33] D. F. Measday, "The nuclear physics of muon capture", Physics Reports, vol. 354 (4-5), pp. 243-409 (2001)
https://www.sciencedirect.com/science/article/pii/S0370157301000126
[34] https://en.wikipedia.org/wiki/Muon_capture

[35] N. C. Mukhopadhyay, “Nuclear Muon Capture”, PHYSICS REPORTS (Section C of Physics Letters) vol. 30(1), pp. 1—144 (1977)
[36] V. C. Zinov, A. D. Konin and A. I. Mukhin, Soviet Journal Nuclear Physics-USSR, vol. 2, p. 613 (1966)
[37] D. F. Measday, “The nuclear physics of muon capture”, Physics Reports, vol. 354, pp. 243–409 (2001)
[38] S. Stanislaus *et al*., “Atomic capture ratios for muons in oxides”, Nuclear Physics A, vol. 475(4), pp.630-641 (1987)
[39] https://en.wikipedia.org/wiki/Stripping_reaction_(physics)
[40] G. R. Satchler, “The Study of Nuclear Collective Motion by Stripping Reactions”, Annals OF Physics, vol. 3, 275-291 (1958)
[41] N. K. Glendenning, “NUCLEAR STRIPPING REACTIONS”, Annual Reviews of Nuclear Science, vol. 13, pp. 191-260 (1633)
[42] J. R. Oppenheimer and M. Phillips, “Note on the transmutation function for deuterons.”, Physical Review, vol. 48(6), p,500 (1395)
[43] S. T. Butler and O. H. Hittmair, “Nuclear stripping reactions”, Horwitz Publications (1957)
[44] D. J. Nagel, “Deuteron Stripping Reactions”, Unpublished (1966) available from the author.
[45] N. K. Timofeyuk and R. C. Johnson, “Theory of deuteron stripping and pick-up reactions for nuclear structure studies”. Progress in Particle and Nuclear Physics, vol. 111, p.103738 (2020)
[46] T. O. Passell, “The Case for Deuteron Stripping with Metal Nuclei as the Source of the Fleischmann–Pons Excess Heat Effect”, J. Condensed Matter Nuclear Science, vol. 15, pp. 288–294 (2015)
[47] M. Davidson, “Off-mass-shell Particles and LENR”, J. Condensed Matter Nuclear Science, vol. 19, pp. 46–55 (2016)
[48] X. Z. Li *et al*., “Resonant Surface Capture Model”, J. Condensed Matter Nuclear Science, vol. 29, pp. 440–452 (2019)
[49] A. Vaswami *et al.*, “Attention Is All You Need”, https://arxiv.org/pdf/1706.03762.pdf?itid=lk_inline_enhanced-template (2017)
[50] J. Rothwell, https://lenr-canr.org/wordpress/?page_id=2988
[51] J. Rothwell, https://www.lenr-forum.com/forum/thread/6953-the-lenr-canr-chatgpt-is-on-line/?pageNo=1